c-di-GMP-linked phenotypes are modulated by the interaction between a diguanylate cyclase and a polar hub protein

Gianlucca G. Nicastro[1], Gilberto H. Kaihami[1], André A. Pulschen[1], Jacobo Hernandez-Montelongo[#2], Ana Laura Boechat[1], Thays de O. Pereira[1], Eliezer Stefanello[1], Pio Colepicolo[1], Christophe Bordi [3] and Regina L. Baldini*[1].

Departamento de Bioquímica, Instituto de Química, Universidade de São Paulo, Brazil [1]; Instituto de Física "Gleb Wataghin", Universidade Estadual de Campinas, Brazil [2]; Laboratoire d'Ingénierie des Systèmes Macromoléculaires, UMR7255 CNRS – Aix Marseille Université, France [3]. [#] Current adress Departamento de Ciencias Matemáticas y Físicas, Facultad de Ingeniería,Universidad Católica de Temuco, La Araucanía, Chile.

Running title: FimV localizes and modulates DgcP activity

* Address correspondence to Regina L. Baldini, baldini@iq.usp.br.
Av. Professor Lineu Prestes, 748 sala 1211, São Paulo-SP, Brazil, 05508-000
Telephone : +55 11 30918992

Abstract

c-di-GMP is a major player in the decision between biofilm and sessile lifestyles. Several bacteria present a large number of c-di-GMP metabolizing proteins, thus a fine-tuning of this nucleotide levels may occur. It is hypothesized that some c-di-GMP metabolizing proteins would provide the global c-di-GMP levels inside the cell whereas others would maintain a localized pool, with the resulting c-di-GMP acting at the vicinity of its production. Although attractive, this hypothesis was yet to be proven in *Pseudomonas aeruginosa*. We found that the diguanylate cyclase DgcP interacts with the cytosolic region of FimV, a peptidoglycan-binding protein involved in type IV pilus assembly. Moreover, DgcP is located at the cell poles in wild type cells, but scattered in the cytoplasm of cells lacking FimV. Overexpression of DgcP leads to the classical phenotypes of high c-di-GMP levels (increased biofilm and impaired motilities) in the wild-type strain, but not in a Δ*fimV* background. Therefore, our findings strongly suggest that DgcP is regulated by FimV and may provide the local c-di-GMP pool that can be sensed by other proteins at the cell pole, bringing to light a specialized function for a specific diguanylate cyclase.

Importance

Bacteria can switch between sessile and motile lifestyles and c-di-GMP is a crucial second messenger for this decision. They present several proteins that can synthetize, degrade and sense this molecule and it is intriguing why so many apparently redundant proteins are needed. An idea is that some of these proteins may act at specific subcellular locations, leading to the formation of localized c-di-GMP pools that may control the assembly and function of polar-localized machineries such as pili and flagella. We found that DgcP, a c-di-GMP synthesizing enzyme, interacts with the type IV pili hub located at the cell poles, and this

interaction modulates c-di-GMP-related phenotypes. Our findings support the hypothesis that c-di-GMP acts on targets near the spot where it is produced.

Introduction

Over the past decades, (3'-5')-cyclic diguanylic acid (c-di-GMP) has been characterized as an important second messenger in bacteria. The concentration of c-di-GMP within the cell is associated with cellular behavior: high c-di-GMP levels are linked to biofilm formation and low levels to the motile planktonic lifestyle (1, 2). This molecule is synthesized from GTP by a class of enzymes known as diguanylate cyclases (DGC) bearing a conserved GGDEF domain (3). The c-di-GMP hydrolysis reaction is performed by phosphodiesterases (PDE) with EAL or HD-GYP domains, which cleave c-di-GMP to pGpG or GMP, respectively (4, 5). Multiple genes coding for the c-di-GMP-metabolizing proteins are found in a variety of bacterial genomes. A puzzling question in the study of c-di-GMP signaling is how the bacterial cell integrates the contributions of multiple c-di-GMP-metabolizing enzymes to mediate its cognate functional outcomes. Merritt and collaborators showed that the *P. aeruginosa* phenotypes controlled by two different DGC have discrete outputs despite the same level of total intracellular c-di-GMP (6). These data support the model in which localized c-di-GMP signaling contributes to the action of proteins involved in the synthesis, degradation, and/or binding to a downstream target (2). Studies of c-di-GMP signaling regulation during the swarmer to stalked-cell transition in *Caulobacter crescentus* also supports this hypothesis. In this dimorphic bacterium, PleD is a DGC that is inactive in swarmer cells and is activated during the swarmer-to-stalked cell differentiation (7, 8). Activation of PleD is coupled to its subcellular localization at the stalk pole, suggesting that PleD activates nearby downstream effectors involved in pole remodeling (9). Opposite to PleD, the EAL domain protein TipF

68 localizes at the swarmer pole, where it contributes to the proper placement of the motor
69 organelle in the polarized predivisional cell (10).

70 Even though a large body of research on c-di-GMP regulation in *P. aeruginosa* is
71 available, it is still unclear whether compartmentalization of c-di-GMP signaling components is
72 required to mediate an appropriate c-di-GMP signal transduction. The genome of *P.*
73 *aeruginosa* strain PA14 presents forty genes coding for proteins associated with c-di-GMP
74 metabolism (11, 12). Some of these proteins were already characterized and a few of them
75 present a specific localization within the cell. For instance, the DGC WspR is associated to
76 contact-dependent response to solid surfaces. Activation of the Wsp system by contact leads
77 to the formation of subcellular clusters of WspR followed by synthesis of c-di-GMP, increasing
78 exopolysaccharide production and biofilm formation (13). The DGC SadC is a central player in
79 Gac/Rsm-mediated biofilm formation (14) and influences biofilm formation and swarming
80 motility via modulation of exopolysaccharide production and flagellar function (15). Recently, it
81 was demonstrated that SadC activity is promoted by membrane association, with the
82 formation of active DGC oligomers (16). The PDE DipA/Pch is essential for biofilm dispersion
83 (17) and promotes c-di-GMP heterogeneity in *P. aeruginosa* population (18). This PDE is
84 partitioned after cell division and is localized to the flagellated cell pole by the chemotaxis
85 machinery. This asymmetric distribution during cell division results in a bimodal distribution of
86 c-di-GMP (18).

87 Previously, we demonstrated that PA14_72420 is an enzymatically active DGC that
88 increased imipenem fitness (19). Although this protein has been the subject of recent
89 publications that named it as DgcP (20), its molecular function has not yet been addressed.
90 Thus, we decided to pursue its role by seeking for DgcP interaction partners that could
91 participate in the same signaling pathway. DgcP was found to interact with the inner

membrane protein FimV, which has a regulatory role in type IV pilus (T4P) function. Moreover, we determined that DgcP localizes to cell poles in a FimV-dependent manner and is more active when the FimV protein is present. We suggest that the DgcP regulation by FimV may provide a local c-di-GMP pool at the cell pole, making this second messenger available for the c-di-GMP binding proteins that may regulate the machineries associated with the cell motility, such as the flagellum and pili.

Results

DgcP interacts with FimV. One of the interesting paradoxes of signal transduction by c-di-GMP is the redundancy of DGCs and PDEs in bacterial cells. It has been shown that distinct phenotypes are controlled by specific DGCs or PDEs (2, 6). The specificity of DGCs and PDEs has been proposed to be related to protein localization, allowing the regulation of subcellular pools of c-di-GMP close to a target receptor (6, 21). Therefore, we sought, using bacterial two-hybrid system, for interaction partners of DgcP that could give a hint of DcgP localization and function. The bait plasmid pKT25_*dgcP* was constructed with the complete *dgcP* coding region (**Fig. 1A**) and co-transformed in BTH101 *E. coli* cells with a *P. aeruginosa* fragment prey library cloned in the pUT18C plasmid (22). About 100,000 co-transformants were obtained and 40 positive red colonies identified. All positives clones were retested by individually transforming different pUT18 derivative preys and the pKT25_*dgcP* or pKT25 empty vector plasmids into BTH101 cells. From the 40 clones initially obtained, 26 were confirmed and the inserts were further identified by DNA sequencing. Only two clones presented *in frame* inserts, one of them corresponding to a short peptide fragment (36 amino acids) of the cytoplasmic, C-terminal portion of FimV (**Fig. 1B,** red box). FimV is a large protein (924 amino acids, 97 kDa) containing a periplasmic domain with a peptidoglycan-binding LysM motif connected via a single transmembrane segment to a highly acidic

cytoplasmic domain with three predicted protein-protein interaction tetratricopeptide repeat (TPR). FimV is part of the T4P secretion machinery in *Pseudomonas* (23) and is required for localization of some T4P assembly components to the cell pole (24). As T4P is important for initial cell attachment and the Δ*dgcP* mutant is impaired in this trait (20), we decided to further investigate the interaction of FimV with DgcP. Two constructions, one containing the FimV cytoplasmic region and the other, a smaller cytoplasmic fragment were cloned into pUT18 plasmid (**Fig. 1B**). After co-transformation of each of these plasmids with pKT25_*dgcP*, we confirmed that DgcP interacts with the cytoplasmic region of FimV (**Fig. 1C** and **D**). Stronger interactions were observed with the constructs containing the prey fragment or the full cytoplasmic region.

DgcP localizes at the cell poles. Type IV pili are surface appendages that localize at the cell poles in *P. aeruginosa*. There are several polar localized proteins involved in the assembly and regulation of the T4P system and FimV is one of them (23, 25, 26). Due to its interaction with FimV, we asked whether DgcP would also localize at the cell poles. Indeed, when cells overexpresses the fusion protein DgcP-msfGFP, polar fluorescent foci were observed in virtually 100% of both PA14 (not shown) and Δ*dgcP* strains (**Fig. 2A**). This localization is lost when DgcP-msfGFP is expressed in a Δ*fimV* mutant, where the fluorescence is scattered throughout the cells (**Fig. 2B and C**). To narrow the DgcP region important to the interaction, we use two different DgcP-msfGFP fusions, one containing the first 199 amino acids (N-ter-DgcP-msfGFP) and the other the last 461 amino acids (C-ter-DgcP-msfGFP) (**Fig. 2A**). The C-terminal fusion fluorescence was scattered in the cells (not show) and cells overexpressing the N-ter-DgcP-msfGFP presented a growth defect, precluding its analysis. Therefore, we cannot determine precisely which region of DgcP is important to polar localization.

As the DgcP C-terminal construct is not localized and there are no predicted domains in the N-terminal region, we aligned 85 sequences of putative DgcP orthologues from 75 species, includind 53 Pseudomonadaceae and 32 other proteobacteria, such as Vibrionales and Alteromonadales (Table S2). We found that the N-terminal region is composed by two separate conserved segments (**Fig. S1**) and both or one of them may be responsible for interaction with FimV, which homologues are present in all those bacterial genomes.

DgcP plays a role in biofilm formation. The role of DgcP in biofilm formation has been investigated by different groups under different conditions. Kulasekara and collaborators showed that mutation in DgcP abolished biofilm formation in LB medium (11) and Ha and collaborators showed that a *dgcP* mutation did not affect biofilm formation in M63 minimum medium (27). Aragon and collaborators demonstrated that deletion of *dgcP* orthologues in *Pseudomonas savastanoi* pv. savastanoi and *P. aeruginosa* PAK indeed decreased biofilm formation in LB (20). Here, we confirmed that the PA14 Δ*dgcP* mutant is impaired in biofilm formation in the rich medium LB, but minor differences were observed in minimal M63 medium (**Fig. 3A**). These results are in agreement with the differences observed by the two previous studies (11, 27). The expression in trans of *dgcP* restores the phenotype of biofilm defect on Δ*dgcP* (**Fig. 3B** and **C**). In LB, Δ*dgcP* was not able to form a biofilm and just a few adherent cells were observed by confocal laser scanning microscopy (CLSM) after 16h post-inoculation, while the wild type PA14 biofilm was mature at this time point (**Fig. 3C**). At 72 hours, Δ*dgcP* biofilm was thin and undifferentiated (**Fig. 3D**). As FimV is also involved in biofilm formation (**Fig. 5**), this is another indication that they have complementary roles in the cells, probably related to the T4P function.

DgcP has a role in twitching motility. *P. aeruginosa* utilizes T4P to move across solid surfaces in a process known as twitching motility. As T4P is regulated by FimV, we decided to

investigate if DgcP is important for twitching. A small portion of the outer edge of the bacterial streak was taken and stabbed into the bottom of the agar plate or placed on a thin layer of solidified media and covered with a glass coverslip. Cells were incubated and active colony expansion occurred at the interstitial interface. Twitching motility was analyzed by staining the plates with crystal violet after 16h (**Fig. 4A** and **B**) or by phase contrast microscopy after 4 hours of colony expansion (**Fig. 4C**). As expected, the Δ*dgcP* mutant presented decreased twitching motility with a less defined structure whereas PA14 presented a well-defined lattice-like network. The *fimV* mutant was not able to perform the twitching motility (**Fig. 4**), as expected. Initiation of biofilm formation was also analyzed after five hours of adhesion of cells on a silicon slide at the air-liquid interface. The cultures were adjusted to an OD_{600} = 0.05 in M63 minimum medium supplemented with glucose and casamino acids. The silicon slide was placed upright in a culture tube and cells at the air-liquid interface were analyzed by field emission scanning electron microscope (FESEM), after different time points (**Fig. 4D**). PA14 early biofilm presented an irregular architecture related to the motility of the initial adhering cells, but only round microcolonies that did not expand on the surface were observed for the Δ*dgcP* mutant (**Fig. 4D**). These results show that DgcP is important to early stages of biofilm formation and twitching motility.

DgcP activity is FimV dependent. Here we observed that the FimV protein localizes the diguanylate cyclase DgcP at the cell pole (**Fig. 2**). Thus, we asked whether DgcP activity could be regulated by FimV. To answer this question, we overexpressed the DgcP-msfGFP in the Δ*fimV* mutant and analyzed the phenotypes related to c-diGMP. Overexpression of the DGCs DgcP and WspR fused to msfGFP in PA14 increases biofilm formation and decreases swimming motility, indicating that these fusions are functional. Both DGCs also complement the Δ*dgcP* mutation, but DcgP-msfGFP is not able to increase biofilm formation or decrease

swimming motility in the Δ*fimV* background, suggesting that it needs FimV for full activity. This is not observed for WspR-msfGFP, which has the same effect with or without FimV in the cells. Overexpression of the C-terminal portion of DgcP (pDgcP-Cterm) that does not localize to the cell poles has no effect in biofilm formation and swimming motility (**Fig. 5A and B**) in all strains tested, even though there is an increase in overall c-di-GMP levels (**Fig. 5C**), suggesting that localization of the diguanylate cyclase activity is important for those phenotypes. Moreover, overexpression of a mutated DgcP in the diguanylate cyclase motif (GGEEF to GGAAF) decreases biofilm formation in the wild type PA14, but has no effect in both Δ*dgcP* and Δ*fimV* backgrounds (**Fig. 5A and B**). DGCs are dimeric proteins therefore the GGAAF mutation may act as a negative dominant on the wild type DgcP.

CdrA is a extracellular protein considered as a scaffold for the biofilm extracellular matrix and transcription of *cdrA* is c-di-GMP-dependent, via FleQ (28) and it is widely used as a reporter of c-di-GMP levels (29). Overexpression of DgcP-msfGFP leads to ~10-fold increased *cdrA* mRNA levels in PA14 and Δ*dgcP*, but only fourfold in the Δ*fimV* strain (**Fig. 5D**).The quantitation of c-di-GMP agrees with the *cdrA* expression levels (**FIG. 5C**). Exopolysaccharide (EPS) is also an indication of c-di-GMP levels in several bacteria (30, 31). DgcP and FimV were overexpressed alone or in combination in *Escherichia coli* cells and the production of EPS was assessed in Congo red plates. FimV overexpression does not result in EPS production, but colonies overexpressing DgcP have a pale tint. When both proteins are overexpressed together, EPS production increases, resulting in pink colonies (**Fig. 5E**). Altogether, our results corroborate the hypothesis that the polar localization of DgcP by FimV also regulates its activity and that DgcP may contribute to a local c-di-GMP pool .

Discussion

Recently, Aragon and collaborators showed that DgcP is a well conserved DGC protein in Pseudomonads related to plant and human infections (20). Previously, we showed that overexpression of this protein alters biofilm formation, swimming and swarming motilities as well as imipenem fitness, due to reduced levels of OprD (19). However, we could not conclude that those phenotypes were specifically related to the physiological role of DgcP, because it was assumed that the overexpression of a DGC increases the global c-di-GMP levels. Herewith, we used protein-protein interactions, characterization of a deletion mutant and protein localization to look for the specific function of DgcP.

P. aeruginosa possesses polar T4P which are used for twitching motility and adhesion (32), essential traits for mature biofilm architecture. Assembly of T4P at normal conditions requires FimV (23), which shares similar domain organization with *Vibrio cholerae* HubP. These proteins, despite low overall sequence similarity, present a conserved N-terminal periplasmic domain required for polar targeting, and a highly variable C-terminal acidic cytoplasmic region, implicated in protein-protein interactions. HubP is required for polar localization of the chromosomal segregation and chemotactic machineries (33, 34). We found that DgcP is present only at the cell poles and that this pattern is dependent on FimV. Thus, we hypothesized that DgcP localization is important for the formation of a localized c-di-GMP pool at the cell poles that would assist the assembly and/or function of the T4P apparatus or other pole-localized organelles (**Fig. 6**). We suggest that DgcP could be one of the sources of c-di-GMP required for pilus biogenesis in *P. aeruginosa* and probably in other gamma-proteobacteria that carry DgcP and FimV homologs.

Assembly of *P. aeruginosa* T4P at normal conditions requires FimX, a polarly localized c-di-GMP binding protein (35) that has degenerate DGC and PDE domains and seems to be

enzymatically inactive (36). It is possible that binding of c-di-GMP to the EAL domain of FimX implicates it as an effector protein rather than a PDE. The FimX homolog in *Xanthomonas citri* interacts with a PilZ protein required for surface localization and assembly of pilin, but does not bind c-di-GMP (37). *X. citri* PilZ subsequently interacts with PilB, an ATPase required for T4P polymerization. This cascade of protein-protein interactions likely conveys the presence of c-di-GMP to PilB, inactivating it and turning motility off (38, 39). Remarkably, suppressor mutations in a *P. aeruginosa fimX* mutant that restored T4P biogenesis and partially restored twitching motility also increased c-di-GMP levels. However, the suppressor mutant cells presented peritrichously localized pili (35), indicating that a more specific source of c-di-GMP would be needed for the correct assembly of the machinery at the cell poles. Similarly, a *P. aeruginosa* PilZ domain protein is also involved in the positive regulation of T4P-based twitching motility and does not bind to c-di-GMP (32), suggesting a conserved mechanism. Cumulatively, these findings imply that the molecular mechanisms of pilus protrusion and retraction are regulated by local fluctuations of c-di-GMP levels. Other polar localized structures, such as flagella and the chemotactic machinery also bind directly or indirectly to c-di-GMP (40, 41), and DgcP may have a function in those mechanisms as well, but further work would be needed to uncover such roles.

P. aeruginosa T4P was demonstrated to be important not only to attach and move, but also to sense mechanical features of the environment. T4P sensing on solid surface increases its extension and retraction frequencies and cAMP production, leading to the upregulation of the cAMP/Vfr-dependent pathway (42). Recently, FimV was associated with this process by interaction with FimL, a scaffold protein that connects T4P with the Chp chemosensory system via interaction with PilG and FimV (25, 26). FimV is also involved in the transcriptional upregulation of *pilY1*, and PilY1 increases the SadC diguanylate cyclase

activity upon surface contact (43). However, SadC presents localized foci at the poles, in the middle of cells and between these two locations (16), suggesting that it may have a broader role. Thus, we suggest that an outside signal could be sensed by T4P and transduced by FimV as described for SadC, resulting in the direct and localized activation of c-di-GMP production by DgcP. The finding that FimV-DgcP interact at the poles is an important step towards the understanding of how c-di-GMP localized pools are formed, controlling the spatial activity of target proteins.

Experimental procedures

Bacterial strains, plasmids and growth conditions. The bacterial strains and plasmids used in the study are described in the Supplementary **Table S2**. For routine cell cultures, bacteria were grown aerobically in Luria–Bertani (LB) broth or LB agar at 37 or 30°C. Ampicillin (100 µg/ ml), kanamycin (50 µg/ml) or gentamicin (10 µg/ml) were added to maintain the plasmids in *E. coli*. Carbenicillin (300 µg/ ml), kanamycin (250 µg/ml) or gentamicin (50 µg/ml) were added to maintain the plasmids in *P. aeruginosa*. For the pJN105 related constructs (**Table S1**), arabinose was added to cultures at 0.2 % final concentration. Both M8 (44) and M63 (45) minimal salt media were supplemented with 1mM $MgSO_4$, 0.2 % glucose and 0.5 % casamino acids (CAA). To visualize bacterial two-hybrid interactions on solid medium, MacConkey indicator medium (Difco) supplemented with 1 % maltose and 100 mM IPTG (Isopropyl β-D-1-thiogalactopyranoside), herein designated MacConkey medium, was used.

General molecular techniques. DNA fragments were obtained by PCR using Q5 DNA polymerase (NEB). Oligonucleotide primers were purchased from Life Technologies and the sequences are listed in **Table S1**. PCR products of the expected sizes were purified from gels using GeneJET TM Gel Extraction Kit (Thermo Scientific), cloned using the SLIC method (46) and transformed into *E. coli* DH5α (**Table S1**). Plasmid purification was performed with GeneJET Plasmid Miniprep kit (Thermo Scientific). Sequencing was carried out using the Big Dye terminator cycle sequencing kit (Applied Biosystems) using the facility of the Departamento de Bioquímica, IQ-USP (SP, Brazil).

To construct unmarked in-frame deletions, the upstream and downstream regions of the target gene were amplified and cloned into the pEX18Ap (*fimV*) or pKNG (*dgcP*). The resulting constructs were used to delete target genes on wild type PA14 genome by

292 homologous recombination. To construct the pDgcP plasmid the *dgcP* coding region was
293 cloned in frame with a synthetic *msfGFP* gene into the pJN105 plasmid. The *msfGFP* codes
294 for a N-terminal 40 amino acids spacer and a C-terminal monomeric super fold GFP. All
295 vectors and constructs are described in more detail in **Table S1**.

296 **Biofilm assays.** Three different biofilm assays were performed. The microtiter dish
297 biofilm formation assay was performed as described (47). The biofilms observed by confocal
298 laser scanning microscopy (CLSM) were grown in 8-well chamber slides and stained with
299 DAPI as described (48) and imaged using a Zeiss - LSM 510-Meta. For the early stages of
300 biofilm formation on silicon wafers, cultures were adjusted to an $O.D_{600}$ = 0.05 in M63 medium
301 and transferred to a 24-well plate where silicon slides (2×1 cm^2) were placed upright in each
302 well. Before using the silicon substrates, they were previously cleaned by ultra-sonication for
303 a period of 15 min each in acetone, isopropanol and distilled water, respectively. Slides were
304 dried under N_2 flow and subsequently treated with O_2 plasma at 100 mTorr for 15 min (720 V
305 DC, 25 mA DC, 18 W; Harrick Plasma Cleaner, PDC-32G). After 60, 180 or 300 minutes the
306 slides were rinsed three times with water, fixed with 4% paraformaldehyde for 1h and
307 analysed by field-emission scanning electron microscopy (FESEM; model F50, FEI Inspect)
308 operated at 2 keV. Prior to examination, samples were coated with sputtered gold to prevent
309 electrical charging.

310 **High-throughput two-hybrid assays.** PAO1 two-hybrid library (22) was tested against
311 the pKT25_DgcP bait. Basically, 25–50 ng of pUT18 library was transformed into BTH101
312 cells carrying the pKT25_DgcP vector and plated on MacConkey medium for 48–96 h at 30
313 °C. Red colonies were picked up and restreaked on MacConkey plates. The positive colonies
314 were cultivated in liquid medium, and plasmids were isolated and further analyzed. The
315 candidate preys were retested individually for interaction with the bait by retransforming

316 pUT18 derivative prey and pKT25 bait plasmids into BTH101 cells and also the pUT18
317 derivative preys and the pKT25 empty vector. The interaction was evaluated by the color of
318 spotted co-transformants on MacConkey plates and β-galactosidase assays. Cells were
319 grown on MacConkey plates for 96 hours and they were scrapped and suspended in 1mL of
320 PBS. 100 µL were used in the classical β-galactosidase assay (49).

321 **Twitching assay.** Macroscopic twitching assay was performed as described (27) with
322 minor modifications. Briefly, a colony was picked with a toothpick and stabbed at the bottom
323 of a plate containing M8 medium supplemented with 1 mM $MgSO_4$, 0.2 % glucose, 0.5 %
324 casamino acids and 2.0 % agar. The plates were incubated upright at 37°C overnight,
325 followed by 48 h of incubation at room temperature (~25°C). Next, the agar was removed,
326 and the bacteria were stained with 0.1% crystal violet. Microscopic twitching assay was
327 performed as described (50).

328 **Swimming assay.** Swimming assays were performed by inoculating 5 µl of a
329 stationary phase-grown liquid cultures in M8 with 0.3% agar that were incubated for 16 h at
330 30°C in a plastic bag to maintain the humidity constant (51).

331 **Congo red assay.** 5 µl of stationary phase-grown cultures were inoculated at 1%
332 agar plates of tryptone broth (10 g/L) containing Congo red (40 µg/mL) and Coomassie
333 brilliant blue (20 µg/mL). The plates were incubated for 16 h at 30°C and then for 96 hours at
334 room temperature.

335 **qRT-PCR.** For qRT-PCRs, total RNA was extracted with Trizol (Invitrogen), treated
336 with DNase I (Thermo Scientific, Waltham, MA, USA) and used for cDNA synthesis with
337 Improm II (Promega) or Superscript III (Invitrogen) and hexamer random primers (Thermo
338 Scientific). cDNA was then amplified with specific primers using Maxima SYBRGreen/ROX

339 qPCR Master Mix (Thermo Scientific) and the 7300 Real Time PCR System (Applied
340 Biosystems). *nadB* was used as internal control for normalization of total RNA levels (52). The
341 relative efficiency of each primer pair was tested and compared with that of *nadB* and the
342 threshold cycle data analysis ($2^{-\Delta\Delta Ct}$) was used (53). All reactions were performed in
343 triplicates, the assays were repeated at least twice using independent cultures and the results
344 of one representative experiment are shown, with average values of technical triplicates and
345 error bars representing standard deviation of ΔΔCt.

346 **Fluorescence and light microscopy.** To verify the localization of DgcP_msfGFP
347 fusions, fluorescence microscopy was performed using a Nikon Eclipse TiE microscope
348 equipped with a 25-mm SmartShutter and an Andor EMCCD i-Xon camera. For fluorescence
349 microscopy and bright field microscopy, a Plan APO VC Nikon 100X objective (NA = 1.4) and
350 a Plan Fluor Nikon 40X objective (NA = 1.3) were used. For membrane staining, cells were
351 treated with 50 µg/mL FM4-64 (Invitrogen). For phase contrast microscopy, a Plan APO λ
352 OFN25 Nikon 100X objective (NA = 1.45) was used. All microscopy assays were performed
353 with immobilized cells on 25 % LB pads with 1.5% agarose. Image analyses were performed
354 using the ImageJ (54) and MicrobeJ (55) softwares.

355 **c-di-GMP extraction and quantification.** c-di-GMP was extracted as described by
356 (56) with minor modifications. 50 mL of cultures were grown in M8 medium at 37°C and 200
357 rpm until reach $O.D._{600}$ = 1. Cells were collected by centrifugation resuspended in 500 µL of
358 M8 medium with 0.6 M perchloric acid. The tubes were incubated on ice for 30 minutes and
359 then centrifuged at 20000 *g* for 10 minutes. The pellets were used for protein quantitation and
360 the supernatants were neutralized with 1/5 volume 2.5 M $KHCO_3$. The nucleotide extracts
361 were centrifuged again and the supernatants were stored at −80 °C. High-performance liquid
362 chromatography (LC) was performed using the 1200 Infinity LC System (Agilent) that consists

of a degasser, a quaternary pump, a thermostated autosampler (4°C) and a temperature (30°C)-controlled column compartment. This system was coupled to an 3200 Qtrap LC-MS/MS system equipped with an Electrospray Ionization source (ESI) (AB Sciex, USA). Analyst 1.4.2 software (AB Sciex, USA) was used to operate the equipment and calculate c-di-GMP concentrations.

Samples (injection of 10 µL) were separated by a Phenomenex Synergi Hydro-RP column (150□×□2 mm, 4 µm) using 0.1% formic acid in 15 mM ammonium acetate as mobile phase A and MeOH as mobile phase B at a flow rate of 0.3 mL min^{-1}. The gradient program was 0 min 2 % B, 0.5 min 2 % B, 4.5 min 30 % B, 6.0 min 80 % B, 7.0 min 80% B, 7.01 min 2% B and 14 min 2 % B. For quantification of c-di-GMP, the tandem mass spectrometry method multiple reaction monitoring (MRM) was used in negative mode. The following parameters were set: nebulizer, heated auxiliary and curtain gases (nitrogen) at 20, 30, 10, respectively; Turbo IonSpray voltage and temperature at -3,800 V and 250 °C, respectively; MRM transition (in m/z) 689.1 → 344.2 with a dwell time of 200 ms per transition; collision energy (CE) at -45 eV; and declustering potential at -53 V. An external standard curve was prepared for c-di-GMP in the MRM mode. The stock solution was diluted and the c-di-GMP peak area plotted against the nominal concentrations (16 to 2,000 ng mL−1).

Multiple Sequence Alignment and secondary structure prediction. Reciprocal best-hit search was performed as described before (Kohler et al., 2015). Briefly, the Kyoto Encyclopedia of Genes and Genomes (KEGG) database was initially used to search open-reading frames showing highest identity against DgcP (GenBank: ABJ14873.1). This search resulted in a list that was used to reciprocal search its highest identity orthologue in *P. aeruginosa* UCBPPA14 genome. In both searches the threshold for Smith-Waterman score was 100, and the resulting best-best hit was filtered using a minimum 20% identity comparing

387 the identified homologue against the DgcP. A list of all organisms that displays a DgcP
388 homologue are listed in Supplemental Table S1. Redundant sequences were filtered using
389 CD-Hit (Li and Godzik, 2006) with a maximum identity of 90% (Supplemental Table S1). A
390 multiple sequence alignment was performed using MUSCLE software (Edgar, 2004). The
391 multiple sequence alignment was then visualized in the jalview (Waterhouse et al., 2009) and
392 secondary structure analysis predicted with JPred (Drozdetskiy et al., 2015).

393 **Acknowledgments.**

394 We would like to thank A. Bisson-Filho for kindly providing the msGFP synthetic gene,
395 D. Schechtman and M. Navarro for carefully reading the manuscript. We are also in debt with
396 F. Gueiros-Filho, L. Zambotti-Villela and M.A. Cotta for assistance with fluorescence
397 microscopy, mass spectrometry and electron microscopy, repectively. We acknowledge the
398 National Nanotechnology Laboratory (LNNano, CNPEM) for granting access to the electron
399 microscopy facilities.

400 Conceived and designed the experiments: GGN, CB and RLB. Performed the FESEM
401 experiments: JHM. Performed two-hybrid screening: GGN and CB. Performed fluorescence
402 and light microscopy: GGN and AAP. General molecular procedures: GGN, GHK, ALB and
403 TOP. HPLC-MS/MS: ES. Contributed reagents/materials/analysis tools: RLB, CB, PC. Wrote
404 the paper: GGN, RLB.

405 G.G.N. is supported by São Paulo Research Foundation (FAPESP) grant numbers:
406 2013/02375-1 and 2014/02381-4.

407 R.L.B. is partially supported by National Council for Scientific and Technological
408 Development (CNPq 307218/2014-7) a São Paulo Research Foundation (FAPESP
409 2014/05082-8).grant allowed the work in RLB laboratory.

C.B. is supported by the ANR grants REGALAD ANR-14-CE09-0005-02.

The authors declare that there is no conflict of interest.

References

1. **Simm R**, **Morr M**, **Kader A**, **Nimtz M**, **Romling U**. 2004. GGDEF and EAL domains inversely regulate cyclic di-GMP levels and transition from sessility to motility. Mol Microbiol **53**:1123–1134.

2. **Romling U**, **Galperin MY**, **Gomelsky M**. 2013. Cyclic di-GMP: the first 25 years of a universal bacterial second messenger. Microbiol Mol Biol Rev **77**:1–52.

3. **Chan C**, **Paul R**, **Samoray D**, **Amiot NC**, **Giese B**, **Jenal U**, **Schirmer T**. 2004. Structural basis of activity and allosteric control of diguanylate cyclase. Proc Natl Acad Sci U S A **101**:17084–17089.

4. **Schmidt AJ**, **Ryjenkov DA**, **Gomelsky M**. 2005. The ubiquitous protein domain EAL is a cyclic diguanylate-specific phosphodiesterase: enzymatically active and inactive EAL domains. J Bacteriol **187**:4774–4781.

5. **Ryan RP**, **Fouhy Y**, **Lucey JF**, **Crossman LC**, **Spiro S**, **He Y-W**, **Zhang L-H**, **Heeb S**, **Camara M**, **Williams P**, **Dow JM**. 2006. Cell-cell signaling in *Xanthomonas campestris* involves an HD-GYP domain protein that functions in cyclic di-GMP turnover. PNAS **103**:6712–6717.

6. **Merritt JH**, **Ha D-G**, **Cowles KN**, **Lu W**, **Morales DK**, **Rabinowitz J**, **Gitai Z**, **O'Toole GA**. 2010. Specific control of *Pseudomonas aeruginosa* surface-associated behaviors by two c-di-GMP diguanylate cyclases. MBio **1**:e00183-10-.

7. **Paul R**, **Weiser S**, **Amiot NC**, **Chan C**, **Schirmer T**, **Giese B**, **Jenal U**. 2004. Cell cycle-dependent dynamic localization of a bacterial response regulator with a novel di-guanylate cyclase output domain. Genes Dev **18**:715–727.

8. **Aldridge P**, **Paul R**, **Goymer P**, **Rainey P**, **Jenal U**. 2003. Role of the GGDEF

regulator PleD in polar development of *Caulobacter crescentus*. Mol Microbiol **47**:1695–1708.

9. **Paul R**, **Abel S**, **Wassmann P**, **Beck A**, **Heerklotz H**, **Jenal U**. 2007. Activation of the diguanylate cyclase PleD by phosphorylation-mediated dimerization. J Biol Chem **282**:29170–29177.

10. **Davis NJ**, **Cohen Y**, **Sanselicio S**, **Fumeaux C**, **Ozaki S**, **Luciano J**, **Guerrero-Ferreira RC**, **Wright ER**, **Jenal U**, **Viollier PH**. 2013. De- and repolarization mechanism of flagellar morphogenesis during a bacterial cell cycle. Genes Dev **27**:2049–2062.

11. **Kulasakara H**, **Lee V**, **Brencic A**, **Liberati N**, **Urbach J**, **Miyata S**, **Lee DG**, **Neely AN**, **Hyodo M**, **Hayakawa Y**, **Ausubel FM**, **Lory S**. 2006. Analysis of *Pseudomonas aeruginosa* diguanylate cyclases and phosphodiesterases reveals a role for bis-(3'-5')-cyclic-GMP in virulence. Proc Natl Acad Sci U S A **103**:2839–2844.

12. **Lee DG**, **Urbach JM**, **Wu G**, **Liberati NT**, **Feinbaum RL**, **Miyata S**, **Diggins LT**, **He J**, **Saucier M**, **Deziel E**, **Friedman L**, **Li L**, **Grills G**, **Montgomery K**, **Kucherlapati R**, **Rahme LG**, **Ausubel FM**. 2006. Genomic analysis reveals that *Pseudomonas aeruginosa* virulence is combinatorial. Genome Biol **7**:R90.

13. **Huangyutitham V**, **Güvener ZT**, **Harwood CS**. 2013. Subcellular clustering of the phosphorylated WspR response regulator protein stimulates its diguanylate cyclase activity. MBio **4**:e00242-13.

14. **Moscoso JA**, **Jaeger T**, **Valentini M**, **Hui K**, **Jenal U**, **Filloux A**. 2014. The diguanylate cyclase SadC is a central player in Gac/Rsm-mediated biofilm formation in *Pseudomonas aeruginosa*. J Bacteriol **196**:4081–4088.

15. **Merritt JH**, **Brothers KM**, **Kuchma SL**, **O'Toole GA**. 2007. SadC reciprocally influences biofilm formation and swarming motility via modulation of exopolysaccharide production and flagellar function. J Bacteriol **189**:8154–8164.

16. **Zhu B**, **Liu C**, **Liu S**, **Cong H**, **Chen Y**, **Gu L**, **Ma LZ**. 2016. Membrane association of SadC enhances its diguanylate cyclase activity to control exopolysaccharides synthesis and biofilm formation in *Pseudomonas aeruginosa*. Environ Microbiol **18**:3440–3452.

17. **Roy AB**, **Petrova OE**, **Sauer K**. 2012. The phosphodiesterase DipA (PA5017) is essential for *Pseudomonas aeruginosa* biofilm dispersion. J Bacteriol **194**:2904–2915.

18. **Kulasekara BR**, **Kamischke C**, **Kulasekara HD**, **Christen M**, **Wiggins PA**, **Miller SI**. 2013. c-di-GMP heterogeneity is generated by the chemotaxis machinery to regulate flagellar motility. Elife **2013**:e01402.

19. **Nicastro GG**, **Kaihami GH**, **Pereira TO**, **Meireles DA**, **Groleau MC**, **Déziel E**, **Baldini RL**. 2014. Cyclic-di-GMP levels affect *Pseudomonas aeruginosa* fitness in the presence of imipenem. Environ Microbiol **16**:1321–1333.

20. **Aragon IM**, **Pérez-Mendoza D**, **Moscoso JA**, **Faure E**, **Guery B**, **Gallegos M-T**, **Filloux A**, **Ramos C**. 2015. Diguanylate cyclase DgcP is involved in plant and human *Pseudomonas spp.* infections. Environ Microbiol **17**:4332–4351.

21. **McDougald D**, **Rice SA**, **Barraud N**, **Steinberg PD**, **Kjelleberg S**. 2012. Should we stay or should we go: mechanisms and ecological consequences for biofilm dispersal. Nat Rev Microbiol **10**:39–50.

22. **Houot L**, **Fanni A**, **de Bentzmann S**, **Bordi C**. 2012. A bacterial two-hybrid genome fragment library for deciphering regulatory networks of the opportunistic pathogen *Pseudomonas aeruginosa*. Microbiology **158**:1964–1971.

23. **Wehbi H**, **Portillo E**, **Harvey H**, **Shimkoff AE**, **Scheurwater EM**, **Howell PL**, **Burrows LL**. 2010. The peptidoglycan-binding protein fimv promotes assembly of the *Pseudomonas aeruginosa* type IV pilus secretin. J Bacteriol **193**:540–550.

24. **Carter T**, **Buensuceso RNC**, **Tammam S**, **Lamers RP**, **Harvey H**, **Howell PL**, **Burrows LL**. 2017. The type IVa Pilus machinery is recruited to sites of future cell division. MBio **8**:e02103-16.

25. **Inclan YF**, **Persat A**, **Greninger A**, **Von Dollen J**, **Johnson J**, **Krogan N**, **Gitai Z**, **Engel JN**. 2016. A scaffold protein connects type IV pili with the Chp chemosensory system to mediate activation of virulence signaling in *Pseudomonas aeruginosa*. Mol Microbiol **101**:590–605.

26. **Buensuceso RNC**, **Nguyen Y**, **Zhang K**, **Daniel-Ivad M**, **Sugiman-Marangos SN**, **Fleetwood AD**, **Zhulin IB**, **Junop MS**, **Howell PL**, **Burrows LL**. 2016. The Conserved tetratricopeptide repeat-containing C-terminal domain of *Pseudomonas aeruginosa* FimV is required for its Cyclic AMP-dependent and -independent functions. J Bacteriol **198**:2263–2274.

27. **Ha D-G**, **Richman ME**, **O'Toole GA**. 2014. Deletion mutant library for investigation of functional outputs of cyclic diguanylate metabolism in *Pseudomonas aeruginosa* PA14. Appl Environ Microbiol **80**:3384–3393.

28. **Borlee BR**, **Goldman AD**, **Murakami K**, **Samudrala R**, **Wozniak DJ**, **Parsek MR**. 2010. *Pseudomonas aeruginosa* uses a cyclic-di-GMP-regulated adhesin to reinforce the biofilm extracellular matrix. Mol Microbiol **75**:827–842.

29. **Rybtke MT**, **Borlee BR**, **Murakami K**, **Irie Y**, **Hentzer M**, **Nielsen TE**, **Givskov M**, **Parsek MR**, **Tolker-Nielsen T**. 2012. Fluorescence-based reporter for gauging cyclic

505 Di-GMP levels in *Pseudomonas aeruginosa*. Appl Environ Microbiol **78**:5060–5069.

506 30. **Chen LH**, **Köseoğlu VK**, **Güvener ZT**, **Myers-Morales T**, **Reed JM**, **D'Orazio SEF**,
507 **Miller KW**, **Gomelsky M**. 2014. Cyclic di-GMP-dependent Signaling Pathways in the
508 Pathogenic Firmicute Listeria monocytogenes. PLoS Pathog **10**:e1004301.

509 31. **Reichhardt C**, **Jacobson AN**, **Maher MC**, **Uang J**, **McCrate OA**, **Eckart M**, **Cegelski**
510 **L**. 2015. Congo red interactions with curli-producing *E. coli* and native curli amyloid
511 fibers. PLoS One **10**:e0140388.

512 32. **Burrows LL**. 2012. *Pseudomonas aeruginosa* twitching motility: type IV pili in action.
513 Annu Rev Microbiol **66**:493–520.

514 33. **Yamaichi Y**, **Bruckner R**, **Ringgaard S**, **Möll A**, **Cameron DE**, **Briegel A**, **Jensen GJ**,
515 **Davis BM**, **Waldor MK**. 2012. A multidomain hub anchors the chromosome
516 segregation and chemotactic machinery to the bacterial pole. Genes Dev **26**:2348–
517 2360.

518 34. **Rossmann F**, **Brenzinger S**, **Knauer C**, **Dörrich AK**, **Bubendorfer S**, **Ruppert U**,
519 **Bange G**, **Thormann KM**. 2015. The role of FlhF and HubP as polar landmark proteins
520 in *Shewanella putrefaciens* CN-32. Mol Microbiol **98**:727–742.

521 35. **Jain R**, **Behrens A-J**, **Kaever V**, **Kazmierczak BI**. 2012. Type IV pilus assembly in
522 *Pseudomonas aeruginosa* over a broad range of cyclic di-GMP concentrations. J
523 Bacteriol **194**:4285–4294.

524 36. **Navarro MVAS**, **De N**, **Bae N**, **Wang Q**, **Sondermann H**. 2009. Structural analysis of
525 the GGDEF-EAL domain-containing c-di-GMP receptor FimX. Structure **17**:1104–1116.

526 37. **Guzzo CR**, **Dunger G**, **Salinas RK**, **Farah CS**. 2013. Structure of the PilZ-FimXEAL-c-
527 di-GMP complex responsible for the regulation of bacterial type IV pilus biogenesis. J

528 Mol Biol **425**:2174–2197.

529 38. **Guzzo CR**, **Salinas RK**, **Andrade MO**, **Farah CS**. 2009. PilZ protein structure and
530 interactions with PilB and the FimX EAL domain: implications for control of type IV pilus
531 biogenesis. J Mol Biol **393**:848–866.

532 39. **Dunger G**, **Guzzo CR**, **Andrade MO**, **Jones JB**, **Farah CS**. 2014. *Xanthomonas citri*
533 subsp. citri type IV pilus is required for twitching motility, biofilm development, and
534 adherence. Mol Plant-Microbe Interact MPMI **27**:1132–1147.

535 40. **Düvel J**, **Bertinetti D**, **Möller S**, **Schwede F**, **Morr M**, **Wissing J**, **Radamm L**,
536 **Zimmermann B**, **Genieser H-G**, **Jänsch L**, **Herberg FW**, **Häussler S**. 2012. A
537 chemical proteomics approach to identify c-di-GMP binding proteins in *Pseudomonas*
538 *aeruginosa*. J Microbiol Methods **88**:229–236.

539 41. **Baker AE**, **Diepold A**, **Kuchma SL**, **Scott JE**, **Ha DG**, **Orazi G**, **Armitage JP**, **O'Toole**
540 **GA**. 2016. A PilZ domain protein FlgZ mediates c-di-GMP-dependent swarming motility
541 control in *Pseudomonas aeruginosa*. J Bacteriol **13**:1837-1846.

542 42. **Persat A**, **Inclan YF**, **Engel JN**, **Stone HA**, **Gitai Z**. 2015. Type IV pili
543 mechanochemically regulate virulence factors in *Pseudomonas aeruginosa*. Proc Natl
544 Acad Sci U S A **112**:7563–7568.

545 43. **Luo Y**, **Zhao K**, **Baker AE**, **Kuchma SL**, **Coggan KA**, **Wolfgang MC**, **Wong GCL**,
546 **O´Toole GA**. 2015. A hierarchical cascade of second messengers regulates
547 *Pseudomonas aeruginosa* Surface Behaviors. MBio **6**:e02456-14.

548 44. **Kohler T**, **Curty LK**, **Barja F**, **van Delden C**, **Pechere JC**. 2000. Swarming of
549 *Pseudomonas aeruginosa* is dependent on cell-to-cell signaling and requires flagella
550 and pili. J Bacteriol **182**:5990–5996.

551 45. **Pardee AB**, **Jacob F**, **Monod J**. 1959. The genetic control and cytoplasmic expression
552 of “inducibility” in the synthesis of b-galactosidase in E. coli. J Mol Biol **1**:165–178.

553 46. **Jeong J-Y**, **Yim H-S**, **Ryu J-Y**, **Lee HS**, **Lee J-H**, **Seen D-S**, **Kang SG**. 2012. One-step
554 sequence- and ligation-independent cloning as a rapid and versatile cloning method for
555 functional genomics studies. Appl Environ Microbiol **78**:5440–5443.

556 47. **O’Toole GA**. 2011. Microtiter Dish Biofilm Formation Assay. J Vis Exp **47**:e2437.

557 48. **Jurcisek J a**, **Dickson AC**, **Bruggeman ME**, **Bakaletz LO**. 2011. *In vitro* biofilm
558 formation in an 8-well chamber slide. J Vis Exp **47**:e2481.

559 49. **Miller JH**. 1972. Experiments in Molecular Genetics, 2nded. Cold Spring Harbor
560 Laboratory, Cold Spring Harbor, New York.

561 50. **Turnbull L**, **Whitchurch CB**. 2014. Motility assay: twitching motility. Methods Mol Biol
562 **1149**:73–86.

563 51. **Ha DG**, **Kuchma SL**, **O’Toole GA**. 2014. Plate-Based assay for swimming motility in
564 *Pseudomonas aeruginosa*. Methods Mol Biol **1149**:59–65.

565 52. **Lequette Y**, **Lee JH**, **Ledgham F**, **Lazdunski A**, **Greenberg EP**. 2006. A distinct QscR
566 regulon in the *Pseudomonas aeruginosa* quorum-sensing circuit. J Bacteriol **188**:3365–
567 3370.

568 53. **Livak KJ**, **Schmittgen TD**. 2001. Analysis of relative gene expression data using real-
569 time quantitative PCR and the 2(-Delta Delta C(T)) Method. Methods **25**:402–408.

570 54. **Schneider CA**, **Rasband WS**, **Eliceiri KW**. 2012. NIH Image to ImageJ: 25 years of
571 image analysis. Nat Methods **9**:671–675.

572 55. **Ducret A**, **Quardokus EM**, **Brun Y V**. 2016. MicrobeJ, a tool for high throughput
573 bacterial cell detection and quantitative analysis. Nat Microbiol **1**:16077.

574 56. **Irie Y**, **Parsek MR**. 2014. LC/MS/MS-based quantitative assay for the secondary

575 messenger molecule, c-di-GMP. Methods Mol Biol **1149**:271–279.

576

Figure Legends

Figure 1. DgcP interacts with FimV. Schematic diagrams of DgcP (**A**) and FimV (**B**), showing the GGDEF domain of DgcP; the transmembrane region (TM), TPR motifs and the LysM domain of FimV. The red box in FimV corresponds to the prey fragment and lines show the regions cloned to confirm the interaction. The *E. coli* host strain BTH101 was cotransformed with pKTA25_DgcP (full length) and pUT18_FimV constructs, as indicated in the figure; the interactions were observed in MacConkey plates as red colonies (**C**) or measured using the β-galactosidase activity as a reporter (**D**).

Figure 2. DgcP localizes at the cell poles in a FimV-dependent manner. msfGFP was fusioned to DgcP full-length (1-670), its N-terminal (1-199) or the C-terminal (209-670) regions, as depicted (A). The full length protein localizes at the cell poles in the Δ*dgcP* background (B, top panels), but deletion of *fimV* leads to a loss of localization (B, bottom panels). The intensity of the GFP fluorescence was measured in 300 cells of each strains and a heat map of DgcP_msfGFP localization was obtained with MicrobeJ, as described in Material and Methods (**C**).

Figure 3. Mutation in *dgcP* affects biofilm formation. PA14 and the Δ*dgcP* strains were inoculated at OD600 = 0.05 in 48 well polystyrene plates in the media shown and kept at 30°C for 16 h without agitation. The medium was discarded and adherent cells were washed and stained with 1% crystal violet, washed and measured at OD = 595 nm (**A**). The same procedure was carried out for the strains overexpressing DgcP in LB with 0.2% arabinose (**B**). 3D pictures resulting from CLSM after 16 h (**C**) and 72 h (**D**) of biofilm formation in LB at 30^{o}C in an 8-well Lab-tek chambered coverglass system.

Figure 4. Δ*dgcP* mutant presents defects related to surface behaviors. Cells were stabbed into the bottom of an agar plate by using a toothpick and incubated upright at 37°C overnight, followed by 48 h of incubation at room temperature, the medium was discarded and adherent cells stained with crystal violet (**A**). Diameter of the twitching colonies was measured in triplicates (**B**). Light microscopy images of PA14 and Δ*dgcP* twitching colonies. Interstitial biofilms formed at the interface between a microscope slide coated in solidified nutrient media (Gelzan Pad) after four hours of colony expansion. The Δ*fimV* mutant was used as a negative control of twitching (**C**). A silicon slide was placed upright in a culture tube and after the different time points cells at the air-liquid interface were washed, fixed and the spread of cells during the initial stages of biofilm formation was observed by FESEM (**D**).

Figure 5. DgcP activity is FimV dependent. Full-length wild type DgcP (pDgcP) or DgcP mutated in its GGDEF domain (pDgcP-GGAAF), only DgcP C-terminal wild-type region (pDgcP-Cterm) and WspR (pWspR) were overexpressed from the pJN105 vector in PA14, Δ*dgcP* and Δ*fimV* backgrounds. Biofilm (**A**), swimming motility (**B**), c-di-GMP quantitation (**C**) and *cdrA* mRNA relative levels (**D**) were assayed. FimV, DgcP or both were expressed in *E. coli* and the EPS production was assessed in Congo red plates (**E**). Data are the means ± SD from three replicates. *, $p<0.05$; **, $p<0.01$; ***, $p<0.001$

Figure 6. Model of FimV-dependent localization and activity of DgcP. In the PA14 wild type strain, DgcP is located at the pole due to interaction with FimV and may contribute to a local c-di-GMP pool (left). In a Δ*fimV* background, DgcP is scattered in the cytoplasm and may have a small contribution to the global c-di-GMP pool (right). FimV, blue boxes; DgcP, green elipses; c-di-GMP, red dots; nucleoid, blue dashed line; T4P, orange wavy lines and flagella, dark green lines.

Figure S1. Multiple Sequence Alignment (MSA) and secondary structure prediction of DgcP homologues. The MSA was generated using Muscle and edited in Jalview. The amino acids residues are colored using the Clustal X colour scheme. Secondary structure prediction was generated using JPred and is displayed as alpha-helixes (red cylinders) and beta-sheets (green arrows) on the top of the alignment. Horizontal black bars represent the two putative N-terminal domains and the blue bar shows the GGDEF C-terminal domain. The orange vertical bar on the left point to Pseudomonas spp. and the purple bar groups other bacteria, as listed in Table S1.

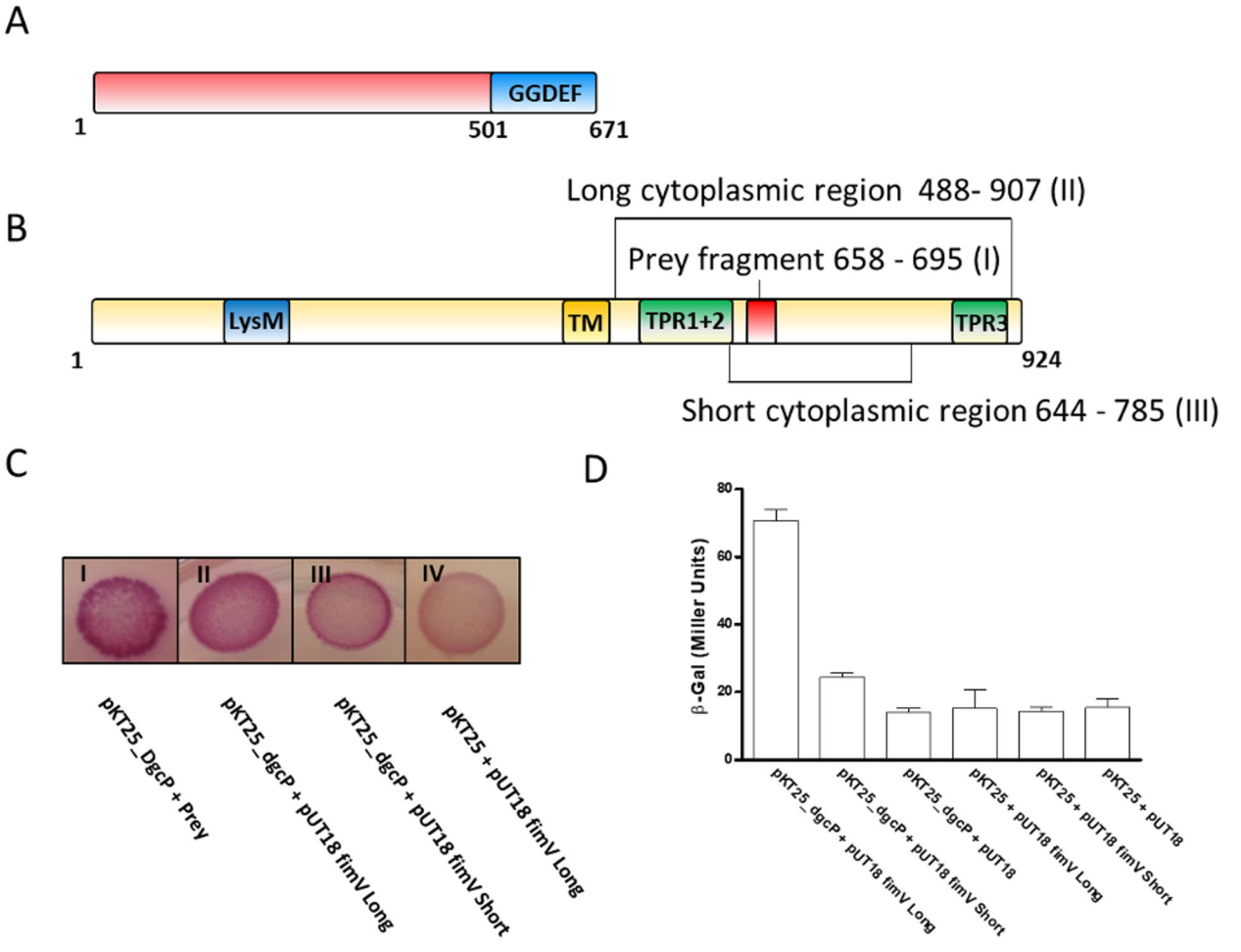
A
GGDEF
1
501
671
B
Long cytoplasmic region 488- 907 (II)
Prey fragment 658 - 695 (I)
LysM
TM
TPR1+2
TPR3
1
924
Short cytoplasmic region 644 - 785 (III)
C
I
II
III
IV
pKT25_DgcP + Prey
pKT25_dgcP + pUT18 fimV Long
pKT25_dgcP + pUT18 fimV Short
pKT25 + pUT18 fimV Long
D
β-Gal (Miller Units)
80
60
40
20
0
pKT25_dgcP + pUT18 fimV Long
pKT25_dgcP + pUT18 fimV Short
pKT25_dgcP + pUT18
pKT25 + pUT18 fimV Long
pKT25 + pUT18 fimV Short
pKT25 + pUT18

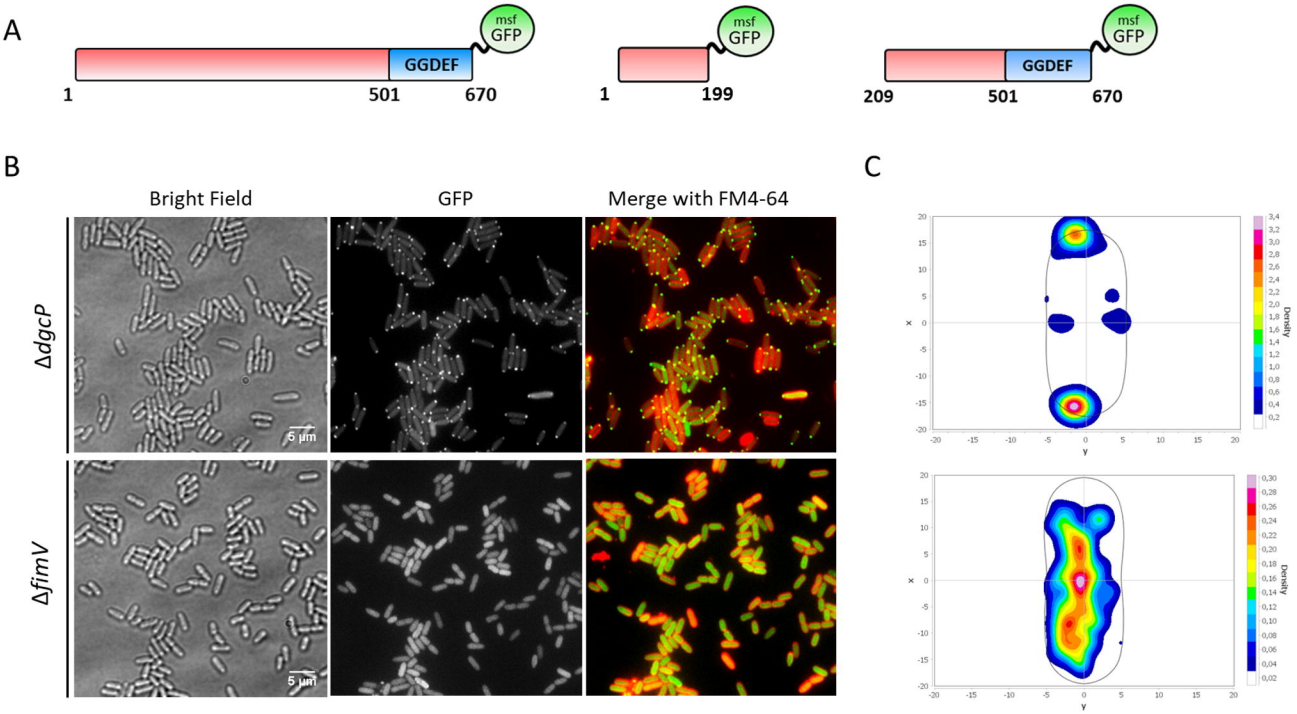
A
msf GFP
GGDEF
1
501
670
msf GFP
1
199
msf GFP
GGDEF
209
501
670
B
Bright Field
GFP
Merge with FM4-64
ΔdgcP
ΔfimV
5 µm
5 µm
C
Density
Density
x
y

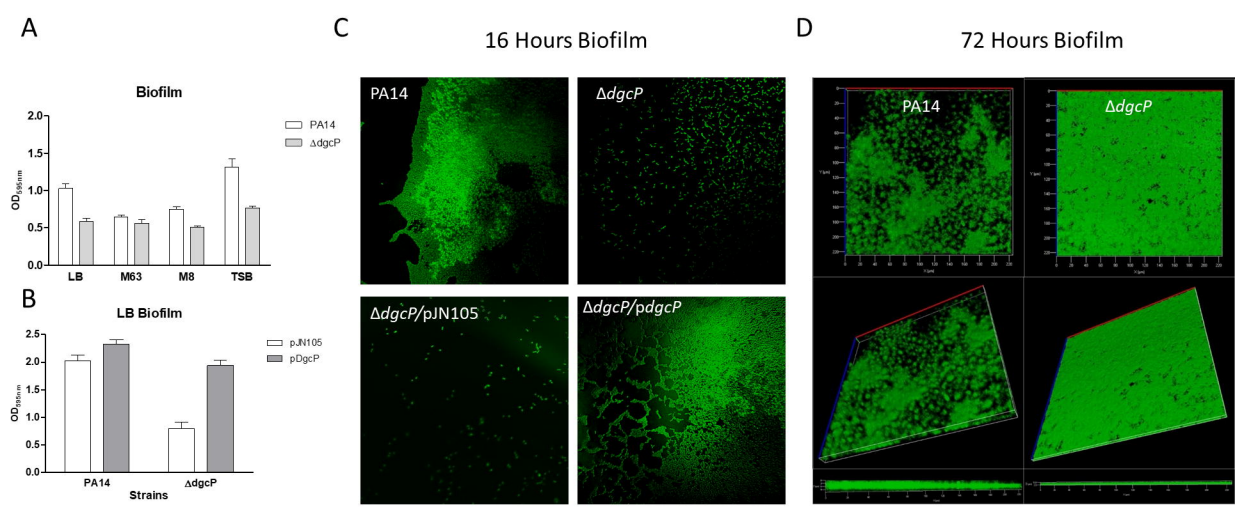
A
Biofilm
PA14
ΔdgcP
OD595nm
2.0
1.5
1.0
0.5
0.0
LB
M63
M8
TSB
B
LB Biofilm
pJN105
pDgcP
OD595nm
2.5
2.0
1.5
1.0
0.5
0.0
PA14
ΔdgcP
Strains
C
16 Hours Biofilm
PA14
ΔdgcP
ΔdgcP/pJN105
ΔdgcP/pdgcP
D
72 Hours Biofilm
PA14
ΔdgcP

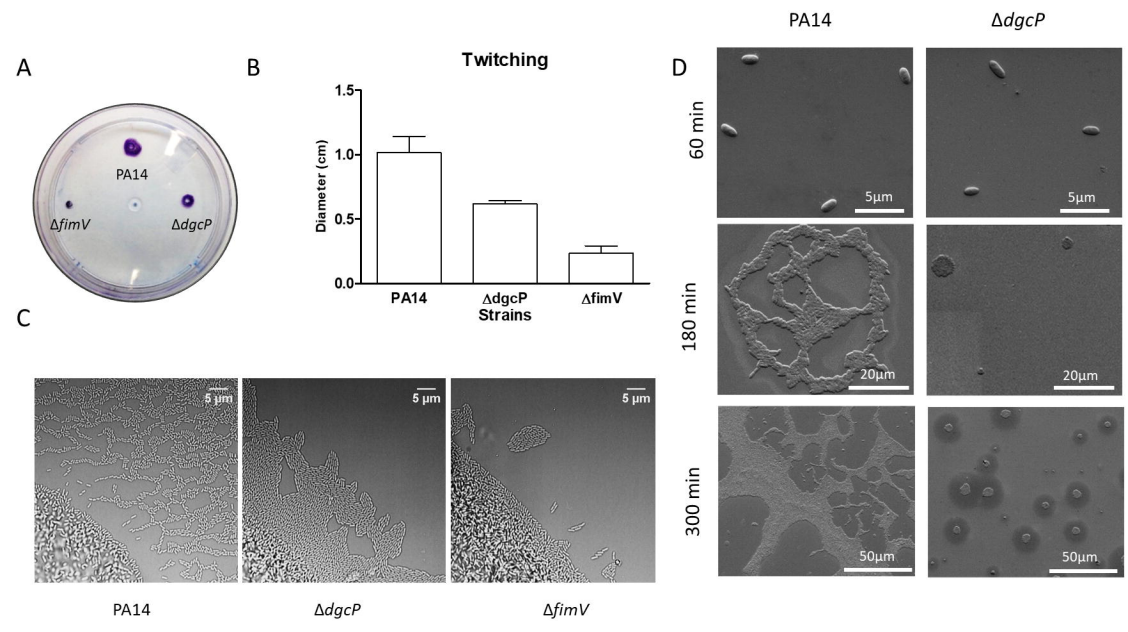
A
PA14
ΔfimV
ΔdgcP
B
Twitching
Diameter (cm)
1.5
1.0
0.5
0.0
PA14
ΔdgcP
ΔfimV
Strains
C
5 μm
5 μm
5 μm
PA14
ΔdgcP
ΔfimV
D
PA14
ΔdgcP
60 min
180 min
300 min
5μm
5μm
20μm
20μm
50μm
50μm

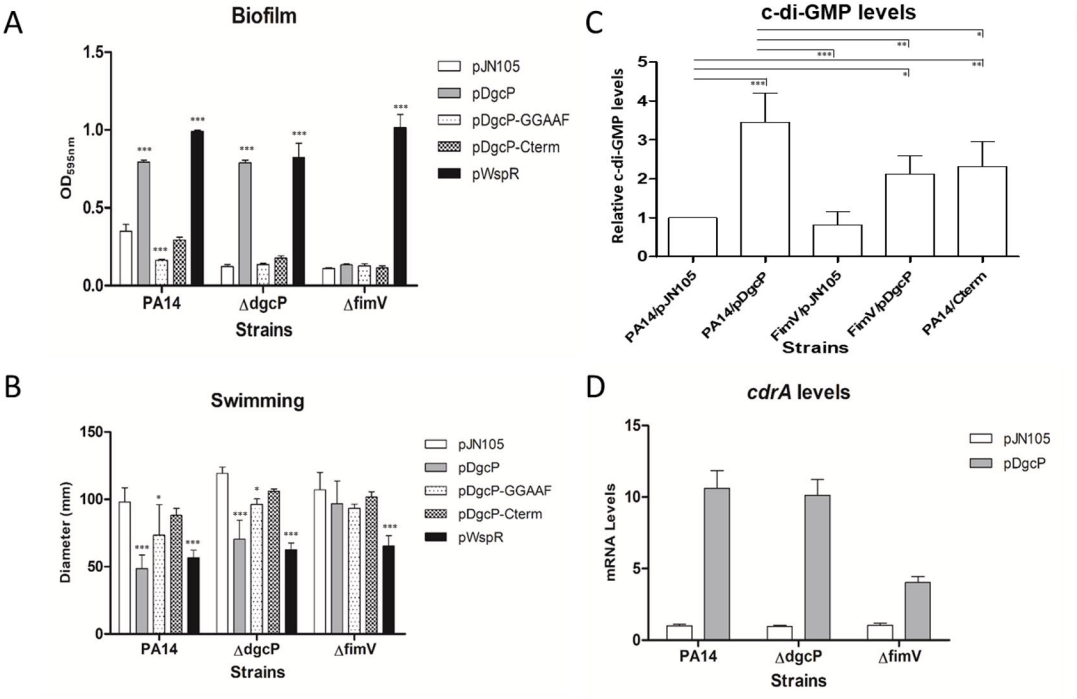
A
Biofilm
1.5
1.0
0.5
0.0
OD595nm
pJN105
pDgcP
pDgcP-GGAAF
pDgcP-Cterm
pWspR
PA14
ΔdgcP
ΔfimV
Strains
B
Swimming
150
100
50
0
Diameter (mm)
pJN105
pDgcP
pDgcP-GGAAF
pDgcP-Cterm
pWspR
PA14
ΔdgcP
ΔfimV
Strains
C
c-di-GMP levels
5
4
3
2
1
0
Relative c-di-GMP levels
PA14/pJN105
PA14/pDgcP
FimV/pJN105
FimV/pDgcP
PA14/Cterm
Strains
D
cdrA levels
15
10
5
0
mRNA Levels
pJN105
pDgcP
PA14
ΔdgcP
ΔfimV
Strains
E
pET-FimV
pET-DgcP
pET-DgcP/FimV

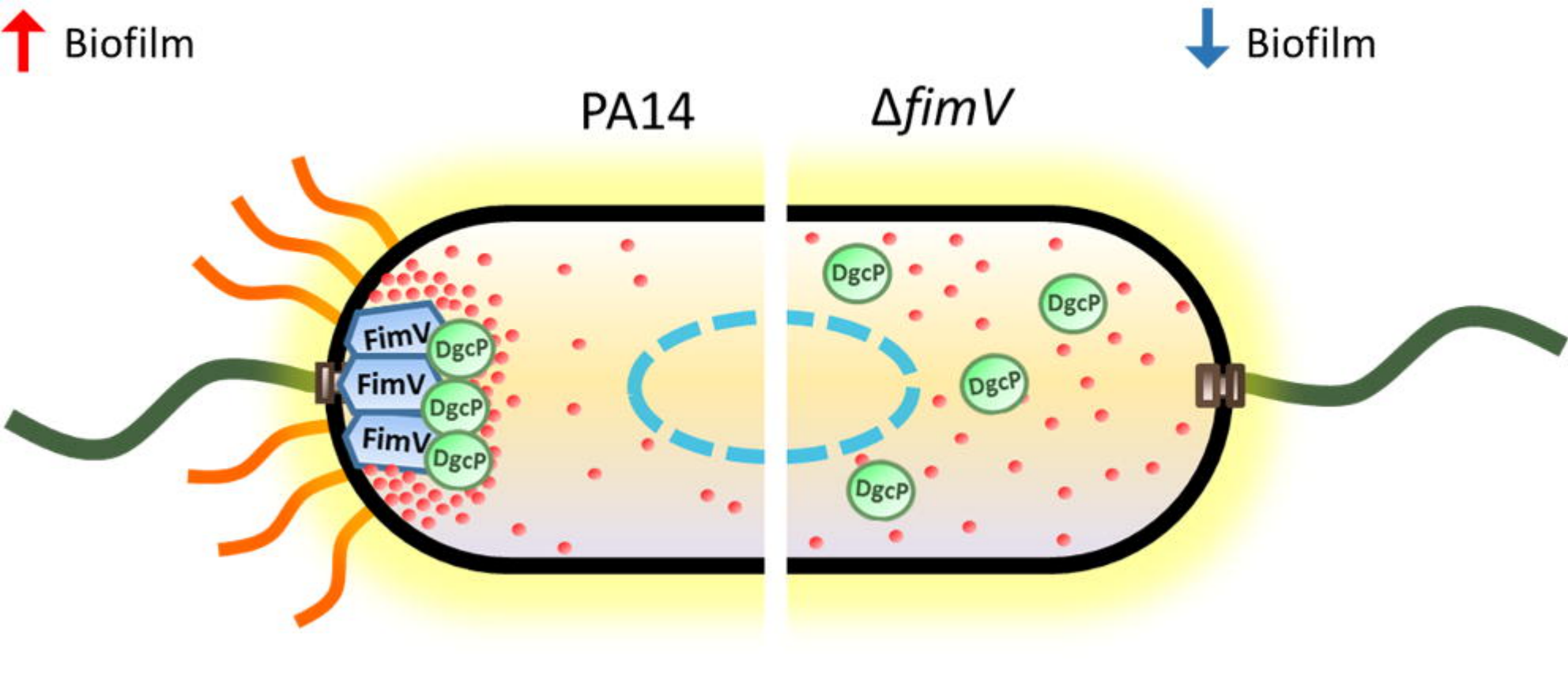
Biofilm
Biofilm
PA14
ΔfimV
FimV
FimV
FimV
DgcP
DgcP
DgcP
DgcP
DgcP
DgcP
DgcP